

Neural Architecture Search From Fréchet Task Distance

Cat P. Le
Duke University
cat.le@duke.edu

Mohammadreza Soltani
Duke University
mohammadreza.soltani@duke.edu

Robert Ravier
Duke University
robert.ravier@duke.edu

Trevor Standley
Stanford University
tstand@cs.stanford.edu

Silvio Savarese
Stanford University
ssilvio@cs.stanford.edu

Vahid Tarokh
Duke University
vahid.tarokh@duke.edu

Abstract

We formulate a Fréchet-type asymmetric distance between tasks based on Fisher Information Matrices. We show how the distance between a target task and each task in a given set of baseline tasks can be used to reduce the neural architecture search space for the target task. The complexity reduction in search space for task-specific architectures is achieved by building on the optimized architectures for similar tasks instead of doing a full search without using this side information. Experimental results demonstrate the efficacy of the proposed approach and its improvements over other methods.

1. Introduction

Most neural architecture search (NAS) methods focus on reducing the complexity of search by using a combination of explicit architecture search domains and specific properties of the given task at hand. This paper is motivated by a common assumption made in transfer and lifelong learning: similar tasks usually have similar neural architectures. Building on this intuition, this paper proposes an algorithm that learns an appropriate architecture for a given task based on its similarity to other learned tasks. To this end, we use the Fréchet task distance, which is an asymmetric distance defined in terms of the Fisher Information Matrix of the loss function with respect to the parameters of the models under consideration. For a target task, the closest task in a given set of baseline tasks is identified and its corresponding architecture is used to construct a neural search space for the target task without requiring prior domain knowledge. Subsequently, the FUSE gradient-based search algorithm [22] is applied to discover an appropriate architecture for the target task. Extensive experimental results for both classification tasks on MNIST [23], CIFAR-10 [21], CIFAR-100 [21], ImageNet [42] data sets, as well as image processing tasks

(e.g., depth estimation, surface normal, etc.) on Taskonomy [54] data set demonstrate the efficacy of our proposed approach in practice.

2. Related Work

Recent NAS techniques have been shown to offer competitive or even better performance to those of hand-crafted architectures. In general, these techniques include approaches based on evolutionary algorithms [41, 49], reinforcement learning [58], and optimization-based approaches [26]. However, many of the existing NAS methods are computationally intense and require thousands of GPU-days operations. To overcome the computational issues and to accelerate the search time complexity, recently, differentiable search methods [7, 27, 34, 28, 52, 50, 2] have been proposed. These methods, together with random search methods and sampling sub-networks from one-shot super-networks [3, 25, 9, 53], can significantly speed up the search time in the neural architecture space [59, 41, 26]. Additionally, random search [24, 25, 44], reinforcement learning with weight-sharing [37, 47, 4], similarity architecture search [22, 32], neural tangent kernel [8], network transformations [5, 12, 20, 18], and few-shot approaches [6, 57, 55, 56] have yielded time-efficient NAS methods.

However, the role of task similarity on the search space of architectures has not been thoroughly considered in the above NAS literature. Intuitively, similar tasks are expected to have similar architectures as manifested by the success of applying transfer learning in many applications [39, 17, 45, 14, 31, 33, 29, 40, 36, 30, 13, 43, 54]. However, the main goal in these works is to transfer trained weights in some previous related tasks to a new one and not to transfer architectures, which are typically fixed. Furthermore, the relationship between visual tasks has been recently investigated in [54, 35, 11, 1, 51]. These works only focus on weight-transfer, and do not utilize task similarities for discovering the high-performing architectures. Finally,

Standley et al. [48] uses brute-force to optimize which tasks should be trained jointly and which should be trained separately in a multi-task learning setting.

It thus makes sense to use the knowledge of architecture(s) of similar tasks as a potential, feasible architecture search space for a new task, and to reduce the dependence on prior domain-knowledge, resulting in reducing the search time for the final architecture.

3. Proposed Approach

In this section, we discuss our proposed approach in two steps. First, we define our task similarity measure and provide some theoretical intuition behind this. Next, we elaborate on the proposed NAS framework based on the task similarity. Through this paper, we denote ℓ_∞ -norm of a matrix B as $\|B\|_\infty = \max_{i,j} |B_{ij}|$. Also, $|S|$ means the size of a set S .

Consider a set A consisting of K baseline tasks T_i and its corresponding data set X_i , denoted jointly by pairs (T_i, X_i) for $i = 1, 2, \dots, K$ where $X_i = X_i^{(1)} \cup X_i^{(2)}$ with $X_i^{(1)}$ and $X_i^{(2)}$ denote the training and the test data, respectively. Below, a NAS framework is presented for finding a well-performing architecture for a target task b , denoted by the pair (T_b, X_b) , based on the knowledge of architectures of these K learned baseline tasks. We assume that $X_i, i = 1, 2, \dots, K$ and X_b are known, and are of the same size. The entire pipeline of the proposed approach, whose pseudo-code is given by Algorithm 1, is given below:

1. **Task Distance.** First, the dissimilarity of each learned task to the target task using the Fréchet distance of Fisher Information Matrices (FIMs) is computed. The closest baseline task based on the computed dissimilarities is returned.
2. **Neural Architecture Search.** Next, a suitable search space for the target task is determined based on the closest task architecture. Subsequently, a search within this space is performed to find a well-performing architecture for the target task b .

3.1. Task Distance

Before discussing the task distance, we recall the definition of the Fisher Information Matrix for a neural network.

Definition 1 (Fisher Information Matrix). *Let N be a neural network with data X , weights θ , and the negative log-likelihood loss function $L(\theta) := L(\theta, X)$. The Fisher Information Matrix is defined as:*

$$F(\theta) = \mathbb{E}[\nabla_\theta L(\theta) \nabla_\theta L(\theta)^T] = -\mathbb{E}[\mathbf{H}(L(\theta))], \quad (1)$$

where \mathbf{H} is the Hessian matrix, i.e., $\mathbf{H}(L(\theta)) = \nabla_\theta^2 L(\theta)$, and expectation is taken w.r.t the distribution of data.

Algorithm 1: NAS framework

Data: $A = \{(T_1, X_1), \dots, (T_K, X_K)\}$,
 $b = (T_b, X_b)$

Input: ε -approximation network, # of candidates C ,
baseline search spaces $\{S_1, \dots, S_K\}$

Output: Best architecture for b

1 **Function** FUSE (*candidates C , data X*) :

2 $\alpha = 1/|C|$

3 Relax the output of C (using Softmax function):

$$\bar{c}(X) = \sum_{c \in C} \frac{\exp(\alpha_c)}{\sum_{c' \in C} \exp(\alpha_{c'})} c(X)$$

4 **while** α not converge **do**

5 Update C by descending $\nabla_w \mathcal{L}_{tr}(w; \alpha, \bar{c})$

6 Update α by descending $\nabla_\alpha \mathcal{L}_{val}(\alpha; w, \bar{c})$

7 **return** $c^* = \operatorname{argmin}_{c \in C} \alpha_c$

8

9 **Function** Main:

10 **for** $i \in (A \cup b)$ **do**

11 Compute Fisher Information Matrix $F_{i,b}$
 using the test data $X_b^{(2)}$

12 **for** $a \in A$ **do**

13 Compute the distance to target task b :

$$d[a, b] = \frac{1}{\sqrt{2}} \|F_{a,b}^{1/2} - F_{b,b}^{1/2}\|_F$$

14 $a^* = \operatorname{argmin}_{a \in A} d[a, b]$

15 Define search space $S = S_{a^*}$

16 **while** criteria not met **do**

17 Sample C candidates $\in S$

18 $c^* = \text{FUSE}((C \cup c^*), X_b)$

19 **return** best architecture c^*

In practice, we use the empirical Fisher Information Matrix computed as follows:

$$\hat{F}(\theta) = \frac{1}{|X|} \sum_{i \in X} \nabla_\theta L^i(\theta) \nabla_\theta L^i(\theta)^T, \quad (2)$$

where $L^i(\theta)$ is the loss value for the i^{th} data for the set X^1 .

As described above, in the first step, we need to find the closest task to the target task from K learned baseline tasks. To this end, we define a dissimilarity measure between tasks based on the Fréchet distance as a function of the Fisher Information Matrix. In particular, let $\mathcal{P}_N(T, X^{(2)}) \in [0, 1]$ be a function that measures the performance of a given architecture N on a task T with the test data set $X^{(2)}$. We have the following definitions:

¹From now on, we use F instead of \hat{F} for the notation simplicity.

Definition 2 (ε -approximation Network). *An architecture N is called an ε -approximation network for (T, X) if it is trained using training data $X^{(1)}$ such that $\mathcal{P}_N(T, X^{(2)}) \geq 1 - \varepsilon$, for a given $0 < \varepsilon < 1$.*

Definition 3 (Structurally-Similar ε -approximation Networks w.r.t. (T, X)). *Two ε -approximation networks N_1 and N_2 are called structurally-similar w.r.t. (T, X) if they have exact architecture (the same number of units, the same number of layers, etc), and they are trained on task T using the training data set $X^{(1)}$.*

Now, suppose that for a given ε , the ε -approximation networks for the learned baseline tasks, (T_i, X_i) for $i = 1, 2, \dots, K$ denoted by N_1, N_2, \dots, N_K , respectively (ε is selected such that $\min_{i \in \{1, 2, \dots, K\}} \mathcal{P}_{N_i}(T_i, X_i^{(2)}) \geq 1 - \varepsilon$). These for example may be networks with well-known hand-designed architectures (e.g., VGG, ResNet, DenseNet for classification tasks). Next, we define the distance between the two tasks.

Definition 4 (Fréchet Task Distance). *Let a and b be two tasks with N_a and N_b denote their corresponding ε -approximation networks, respectively. (i.e., N_a and N_b are trained with their own data sets to achieve high performance). Let $F_{a,b}$ be the Fisher Information Matrix of N_a with the data set $X_b^{(2)}$ from the task b , and $F_{b,b}$ be the Fisher Information Matrix of N_b with the data set $X_b^{(2)}$ from the task b . We define the distance from the task a to the task b based on Fréchet distance as follows:*

$$d[a, b] = \frac{1}{\sqrt{2}} \text{tr} \left(F_{a,b} + F_{b,b} - 2(F_{a,b} F_{b,b})^{1/2} \right)^{1/2}, \quad (3)$$

where tr denotes the trace of a matrix.

In this paper, we use the diagonal approximation of Fisher Matrices to get around of computational issues of computing the giant full Fisher Matrix. We also normalize them to have a unit trace. As a result, the Fréchet distance in (3) can be simplified as follows:

$$\begin{aligned} d[a, b] &= \frac{1}{\sqrt{2}} \left\| F_{a,b}^{1/2} - F_{b,b}^{1/2} \right\|_F \\ &= \frac{1}{\sqrt{2}} \left[\sum_i \left((F_{a,b}^{ii})^{1/2} - (F_{b,b}^{ii})^{1/2} \right)^2 \right]^{1/2}, \quad (4) \end{aligned}$$

where F^{ii} is the i^{th} diagonal entry of the Fisher Information Matrix. This dissimilarity measure ranges from 0 to 1, with the distance $d = 0$ denotes a perfect similarity and the distance $d = 1$ indicates a perfect dissimilarity. Note that this dissimilarity is inherently *asymmetric* since it might be easier to transfer the knowledge of a complex task to a simple task, but not vice versa. Next, we present some theoretical justification for our measure of similarity. Our goal is

to evaluate how well the baseline approximation networks perform on the target task's data set X_b .

We first note to an immediate observation: If we train any pair of structurally-similar ε -approximation networks w.r.t some target (T, X) with the same conditions (i.e., same initialization, batch order, etc), the Fréchet distance between this pair of networks using the test data set $X^{(2)}$ will be zero. Formally, we have the following proposition:

Proposition 1. *Let X be the data set for the target task T . For any pair of structurally-similar ε -approximation network w.r.t (T, X) using the full or stochastic gradient descent algorithm with the same initialization settings, learning rate, and the same order of data batches in each epoch for the SGD algorithm, the Fréchet distance between the above pair of ε -approximation networks is always zero.*

Proof of Proposition 1. Let N_1 and N_2 be two structurally-similar ε -approximation network w.r.t (T, X) trained using the full or stochastic gradient descent algorithm. According to the Definition 3 and assumptions in the proposition, the Fisher Information Matrix of N_1 and N_2 are the same; hence, the Fréchet distance is zero. \square

In the previous proposition, all the training settings were assumed to be the same for two structurally-similar ε -approximation networks w.r.t (T, X) . However, an important question is whether the Fréchet distance is still a *well-defined* measure regardless of the initial settings, learning rate, and the order of data batches. That is, if we train two structurally-similar ε -approximation network w.r.t (T, X) using SGD with different settings, will the Fréchet distance between N_1 and N_2 , as defined in Equation (4), be (close) zero? We answer this question affirmatively assuming a strongly convex loss function. To this end, we invoke Polyak and Juditsky theorem [38] on the convergence of the average sequence of estimation in different epochs from the SGD algorithm. While the loss function in a deep neural network is not a strongly convex function, establishing the fact that the Fréchet distance is mathematically well-defined even for this case is an important step towards the more general case in a deep neural network and a justification for the success of our empirical study. In addition, there are some recent works that try to establish Polyak and Juditsky theorem for the convex or even some non-convex functions in an asymptotic way [15]. Here, we rely only on the asymptotic version of the theorem proposed originally by [38]. We recall the definition of the strongly convex function.

Definition 5 (Strongly Convex Function). *A differentiable function $f : \mathbb{R}^n \rightarrow \mathbb{R}$ is strongly convex if for all $x, y \in \mathbb{R}^n$ and some $\mu > 0$, we have:*

$$f(y) \geq f(x) + \nabla(f)^T(y - x) + \mu \|y - x\|_2^2. \quad (5)$$

We next state our first theorem. Due to space limitation, we present the proof of Theorems 1 and 2 in the appendix.

Theorem 1. Let X be the data set for the target task T . Consider two structurally-similar ε -approximation networks w.r.t. (T, X) , N_1 and N_2 with the set of weights θ_1 and θ_2 trained using the SGD algorithm where a diminishing learning rate is used for updating weights. Assume that the loss function L for the task T is strongly convex, and its 3rd-order continuous derivative exists and bounded. Let the noisy gradient function in training N_1 and N_2 networks using SGD algorithm be given by:

$$g(\theta_{it}, \epsilon_{it}) = \nabla L(\theta_{it}) + \epsilon_{it}, \text{ for } i = 1, 2, \quad (6)$$

where θ_{it} is the estimation of the weights for network N_i at time t , and $\nabla L(\theta_{it})$ is the true gradient at θ_{it} . Assume that ϵ_{it} satisfies $\mathbb{E}[\epsilon_{it} | \epsilon_{i0}, \dots, \epsilon_{it-1}] = 0$, and satisfies $s = \lim_{t \rightarrow \infty} \|\epsilon_{it} \epsilon_{it}^T | \epsilon_{i0}, \dots, \epsilon_{it-1}\|_\infty < \infty$ almost surely (a.s.). Then the Fréchet distance between N_1 and N_2 computed on the average of estimated weights up to the current time t converges to zero as $t \rightarrow \infty$. That is,

$$d_t = \frac{1}{\sqrt{2}} \left\| \bar{F}_{1t}^{1/2} - \bar{F}_{2t}^{1/2} \right\|_F \xrightarrow{\mathcal{D}} 0, \quad (7)$$

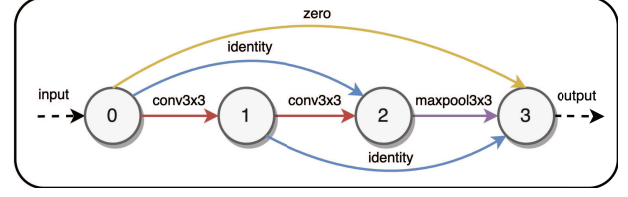
where $\bar{F}_{it} = F(\bar{\theta}_{it})$ with $\bar{\theta}_{it} = \frac{1}{t} \sum_t \theta_{it}$, for $i = 1, 2$.

In our experiments, we found out that the weight averages $\bar{\theta}_{it}$, $i = 1, 2$ can be replaced with only their best estimates for θ_{it} , $i = 1, 2$, respectively. Next, we show that the Fréchet distance is also a well-defined measure between two task-data set pairs. In other words, the Fréchet (asymmetric) distance from the task (T_A, X_A) to the task (T_B, X_B) approaches a constant value regardless of the initialization, learning rate, and the order of data batches in the SGD algorithm provided that X_A and X_B have the same distribution.

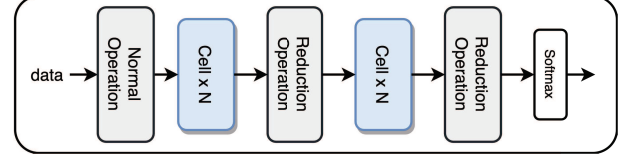
Theorem 2. Let X_A be the data set for the task T_A with the objective function L_A , and X_B be the data set for the task T_B with the objective function L_B . Assume X_A and X_B have the same distribution. Consider an ε -approximation network N trained using both data sets $X_A^{(1)}$ and $X_B^{(1)}$ respectively with the objective functions L_A and L_B to result weights θ_{A_t} and θ_{B_t} at time t . Under the same assumptions on the moment of gradient noise in SGD algorithm and the loss function stated in Theorem 1, the Fréchet distance from the task A to the task B computed from the Fisher Information Matrix of the average of estimated weights up to the current time t converges to a constant as $t \rightarrow \infty$. That is,

$$d_t = \frac{1}{\sqrt{2}} \left\| \bar{F}_{A_t}^{1/2} - \bar{F}_{B_t}^{1/2} \right\|_F \xrightarrow{\mathcal{D}} \frac{1}{\sqrt{2}} \left\| F_A^{*1/2} - F_B^{*1/2} \right\|_F, \quad (8)$$

where \bar{F}_{A_t} is given by $\bar{F}_{A_t} = F(\bar{\theta}_{A_t})$ with $\bar{\theta}_{A_t} = \frac{1}{t} \sum_t \theta_{A_t}$, and \bar{F}_{B_t} is defined in an analogous manner.



(a) A cell structure



(b) A skeleton structure

Figure 1: An example of the cell and the skeleton from a search space of classification tasks.

3.2. Neural Architecture Search

In an analogous manner to recent NAS techniques [27, 10], our architecture search space is defined by cells and skeletons. A cell, as illustrated in Figure 1a, is a densely connected directed-acyclic graph (DAG) of nodes, where nodes are connected by operations. The operations (e.g., identity, zero, convolution, pooling) are normally set so that the dimension of the output is the same as that of the input. Additionally, a skeleton, as illustrated in Figure 1b, is a structure consisting of multiple cells and other operations stacked together, forming a complete architecture. In our framework, the search space for the task is defined in terms of the cells and operations of the closest baseline task. For example, consider a search space whose each cell has n nodes and m possible operations. The total number of possible cells in this space is given by: $m \times \exp\left(\frac{n!}{2(n-2)!}\right)$.

For finding the best candidate, the Fusion Search (FUSE) algorithm [22], as demonstrated in Algorithm 1, is applied to the restricted search space of the closest task. In each iteration, FUSE evaluates a predefined number of network candidates, which are randomly sampled from the search space. This search algorithm considers these candidates as a whole by relaxing their outputs, and performs the optimization using gradient descent. Since the architecture search space is restricted only to the space of the most related task, the search algorithm performs efficiently and requires fewer computational resources as it is demonstrated in our experiments.

4. Experimental Study

In this section, we present our experimental study on various data sets. In particular, we first apply our Fréchet task distance on different classification tasks on MNIST [23],

CIFAR-10 [21], CIFAR-100 [21], ImageNet [42] data sets, and the image processing tasks on Taskonomy [54] data set. For each task, we consider a balanced training data set. That is, except for the classification tasks with all the labels, only a subset of the original training data set is used such that the number of training samples across all the class labels to be equal. Next, we utilize our NAS framework in Algorithm 1 for all the classification tasks. That is, we perform the architecture search for the target task using the search space of the most related task, then compare our optimal network with state-of-art hand-designed architectures and random search approach in terms of the test accuracy, the number of parameters, and the GPU days. In our experiment, the random search algorithm is applied to the reduced search space from the closest task to the target task.

In order to show that our task distance is independent of the choice of ε -approximation networks, (i.e., the consistency of our measure), for the classification tasks, we use 3 widely-used and high-performance architectures as the ε -approximation networks, including VGG-16 [46], ResNet-18 [16], DenseNet-121 [19]. Additionally, we use a deep autoencoder as the ε -approximation network for image processing tasks. To make sure that our results are statistically significant, we run our experiments 10 times with the ε -approximation network being initialized with a different random seed each time and report the mean value as the computed distance.

In the next section, we start with experiments related to classification tasks defined on the MNIST data set.

4.1. MNIST

First, we define four tasks on the MNIST [23] data set. Task 0 and 1 are the binary classification tasks of detecting digits 0 and 6, respectively. Task 2 is a 5-class classification of detecting digits 0, 1, 2, 3, and anything else. Task 3 is the full 10 digits classification. Figure 2 illustrates the mean (the top row) and standard deviation (the bottom row) tables of the distances between each pair of tasks after 10 trial runs with different initial settings. In this Figure, the columns of all tables denote the target task and the rows represent the source tasks. In particular, column i of the mean table indicates the distance to the target task i . We use the mean values as the final task distance between the source and target tasks. The leftmost column is the experiment with the VGG-16 model as the ε -approximation network, while the middle and the third columns are the experiments with the ResNet-18 and DenseNet-121 ones. Our results suggest that Task 0 and 1 are highly related, and Task 3 is the closest task to Task 2. As we can see, although the task distance values depend on the used ε -approximation architecture, the trend remains the same across all 3 architectures. In addition, the standard deviation values in the bottom row of Figure 2 suggest that the computed task distance is stable as the fluc-

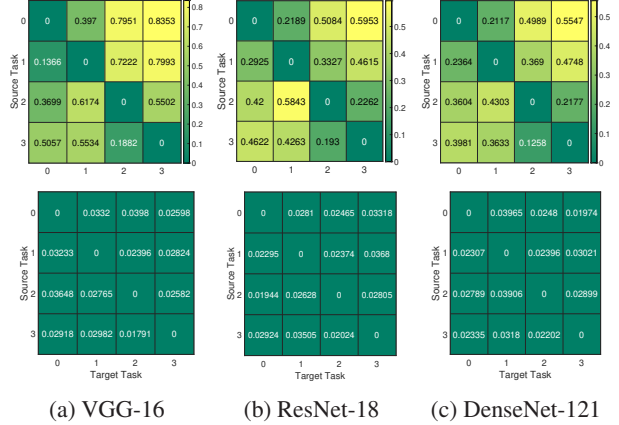


Figure 2: Distance from source tasks to the target tasks on MNIST. The top row shows the mean values and the bottom row denotes the standard deviation of distances between classification tasks over 10 different trials.

Table 1: Comparison of our proposed NAS framework with the hand-designed image classifiers and the random search method on MNITS data set for the target Task 2.

| Architecture | Accuracy | Params (M) | GPU days |
|--------------------|----------|------------|----------|
| VGG-16 [46] | 99.41 | 14.72 | - |
| ResNet-18 [16] | 99.47 | 11.44 | - |
| DenseNet-121 [19] | 99.61 | 6.95 | - |
| Random Search | 99.52 | 2.12 | 4 |
| Our NAS framework* | 99.66 | 2.09 | 2 |

tuations over the mean values do not show any overlap with each other.

Next, we consider the problem of learning architecture for the target Task 2, using the other aforementioned tasks as our baseline tasks. It is observed that Task 3 is the closest one to Task 2. Thus, we apply cell structure and the operations of Task 3 to generate a suitable search space for the target task. The results in Table 1 show the best test accuracy of the optimal architecture found by our framework after 200 iterations compared to a random search algorithm and state-of-art handcrafted networks. The architecture discovered by our framework is competitive with these networks while it results in a significantly smaller amount of parameters.

4.2. CIFAR-10 and CIFAR-100

In this section, we present our experiments on CIFAR-10 and CIFAR-100. First, we define four tasks in the CIFAR-10 [21] data set. Task 0 is a binary classification of indicating 3 objects: automobile, cat, ship (i.e., the goal is to de-

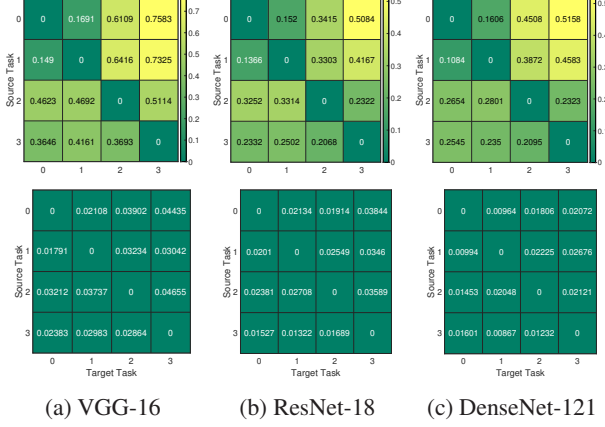


Figure 3: Distance from source tasks to the target tasks on CIFAR-10. The top row shows the mean values and the bottom row denotes the standard deviation of distances between classification tasks over 10 different trials.

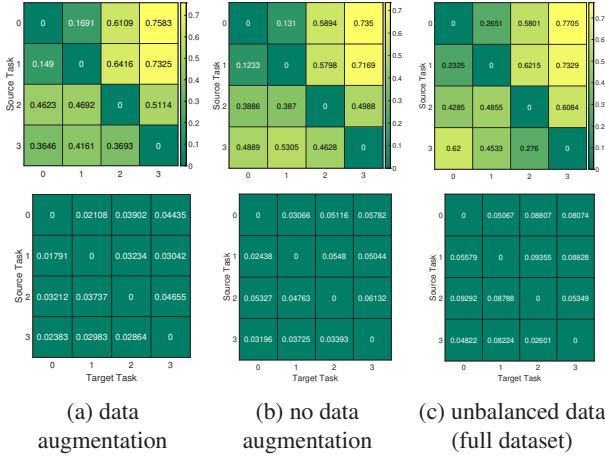


Figure 4: The effect of different initial settings on computing distance between tasks defined on CIFAR-10 data set using VGG-16. as the ϵ -approximation network. The top row shows the mean values and the bottom row denotes the standard deviation of distances over 10 different trials.

cide if the given input image consists of one of these three objects or not). Task 1 is analogous to Task 0 but with different objects: cat, ship, truck. Task 2 is a 5-class classification with labels bird, frog, horse, and anything else. Task 3 is the standard 10 objects classification. Figure 3 illustrates the mean and standard deviation of the distance between CIFAR-10 tasks over 10 trial runs, using 3 different architectures. Additionally, in Figure 4, we study the effect of different initial settings, such as training with/without data augmentation, or using unbalanced data set for the above four tasks on the CIFAR-10 data set and using VGG-16 as the ϵ -approximation network. As we can see in both Fig-

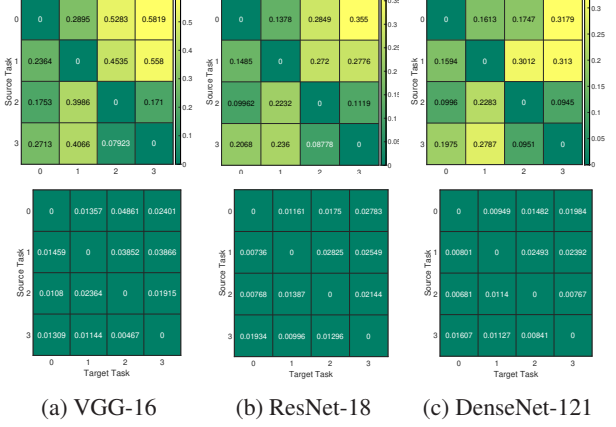


Figure 5: Distance from source tasks to the target tasks on CIFAR-100. The top row shows the mean values and the bottom row denotes the standard deviation of distances between classification tasks over 10 different trials.

Table 2: Comparison of our proposed NAS framework with the hand-designed image classifiers and the random search method on CIFAR10 data set for the target Task 2.

| Architecture | Accuracy | Params (M) | GPU days |
|-------------------|----------|------------|----------|
| VGG-16 [46] | 86.75 | 14.72 | - |
| ResNet-18 [16] | 86.93 | 11.44 | - |
| DenseNet-121 [19] | 88.12 | 6.95 | - |
| Random Search | 88.55 | 3.65 | 4 |
| Our NAS approach* | 90.87 | 3.02 | 2 |

Table 3: Comparison of our proposed NAS framework with the hand-designed image classifiers and the random search method on CIFAR-100 data set for the target Task 2.

| Architecture | Accuracy | Params (M) | GPU days |
|-------------------|----------|------------|----------|
| VGG-16 [46] | 83.93 | 14.72 | - |
| ResNet-18 [16] | 84.56 | 11.44 | - |
| DenseNet-121 [19] | 88.47 | 6.95 | - |
| Random Search | 88.55 | 3.54 | 5 |
| Our NAS approach* | 90.32 | 3.37 | 4 |

ures 3 and 4, the closest tasks to target tasks (columns) in all the tables always result in a unique task no matter what ϵ -approximation network or initial settings we choose.

Similarly, we define four tasks in the CIFAR-100 [21] data set, consisting of 100 objects equally distributed in 20 sub-classes (e.g., vehicles 1, vehicles 2, household furni-

ture, household device, etc). Hence, each sub-class has 5 types of objects. We define Task 0 as a binary classification of detecting an object that belongs to vehicles 1 and 2 sub-classes or not (i.e., the goal is to decide if the given input image consists of one of these 10 vehicles or not). Task 1 is analogous to Task 0 but with different sub-classes: household furniture and devices. Task 2 is a multi-classification with 11 labels defined on vehicles 1, vehicles 2, and anything else. Finally, Task 3 is defined similarly to Task 2; however, with the 21-labels in vehicles 1, vehicles 2, household furniture, household device, and anything else. Figure 5 illustrates the mean and the standard deviation of the distance from the above four source (rows) tasks to the four target (columns) ones after 10 trial runs using 3 different ε -approximation networks.

Next, we consider the problem of searching for a high-performing and efficient architecture for Task 2 in CIFAR-10, and Task 2 in CIFAR-100 data sets. Results in Table 2 and 3 suggest that the constructed architectures for these tasks have higher test accuracy with a fewer number of parameters compared to other approaches.

4.3. ImageNet

For the experiments in this section, we define four multi-classification tasks using 10 labels in ImageNet [42] data set from each we consider 1000 images (800 for training and 200 for the test samples). The list of 10 labels in Task 0 includes tench, English springer, cassette player, chain saw, church, French horn, garbage truck, gas pump, golf ball, parachute. Task 1 is similar to Task 0; however, instead of 3 labels of tench, golf ball, and parachute, it has samples from the grey whale, volleyball, umbrella classes. In Task 2, we also replace 5 labels of grey whale, cassette player, chain saw, volleyball, umbrella in Task 0 with another 5 labels given by platypus, laptop, lawnmower, baseball, cowboy hat. Lastly, Task 3 is defined as a classification task with samples from the following classes: analog clock, candle, sweatshirt, birdhouse, ping-pong ball, hotdog, pizza, school bus, iPod, beaver. The mean and standard deviation tables of the distances between ImageNet tasks for 10 trials with 3 ε -approximation networks are illustrated in Figure 6. Again, it is observed that the order of the distance between the source (rows) and target tasks (columns) remains the same regardless of the choice of ε -approximation networks.

Next, we consider Task 1 as the target task, and our goal is to find an efficient architecture with high test accuracy. Based on the computed distances, we use Task 0 as the closest source task to our target task. As result, we search on the space of this source task. Table 4 presents results indicating that the constructed architecture for the target Task 1 has higher test accuracy with a significantly fewer number of parameters compared to the random search and other hand-designed models. Our experiments suggest that the

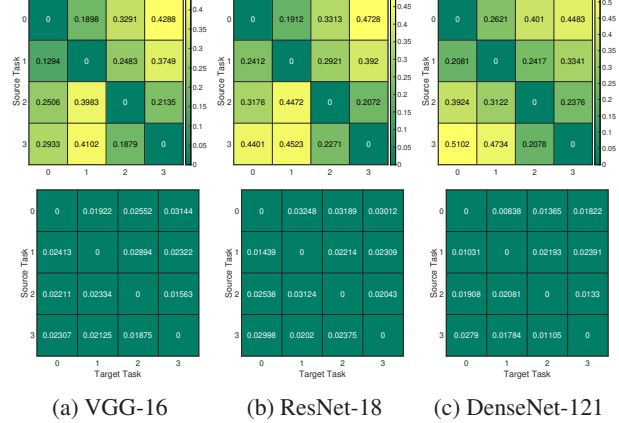


Figure 6: Distance from source tasks to the target tasks on ImageNet. The top row shows the mean values and the bottom row denotes the standard deviation of distances between classification tasks over 10 different trials.

Table 4: Comparison of our proposed NAS framework with the hand-designed image classifiers and the random search method on ImageNet data set for the target Task 1.

| Architecture | Accuracy | Params (M) | GPU days |
|--------------------|----------|------------|----------|
| VGG-16 [46] | 89.88 | 14.72 | - |
| ResNet-18 [16] | 91.14 | 11.44 | - |
| DenseNet-121 [19] | 94.76 | 6.95 | - |
| Random Search | 95.02 | 3.78 | 5 |
| Our NAS approach * | 95.07 | 3.53 | 4 |

proposed framework can utilize the knowledge of the most similar task in order to find a high-performing architecture for the target task with a fewer number of parameters.

4.4. Taskonomy

In this section, we compare our task distance with the one proposed by the Taskonomy paper [54] using the Taskonomy data set[54]. This data set is a collection of 512×512 colorful images of varied indoor scenes. It provides the pre-processed ground truth for 25 vision tasks including semantic and low-level tasks. In this experiment, we consider a set of 10 tasks, including: (0) Euclidean distance, (1) z-depth, (2) 3D-edge, (3) 2D-edge (4) 2D-keypoint, (5) 3D-keypoint, (6) surface normal, (7) curvature, (8) reshading, (9) autoencoding. Please see [54] for detailed task descriptions. For each task, there are 40,000 training samples and 10,000 test samples. Additionally, an autoencoder architecture, including several convolutional and linear layers, with a total of 50.51M parameters is chosen to be the ε -approximation network for all tasks.

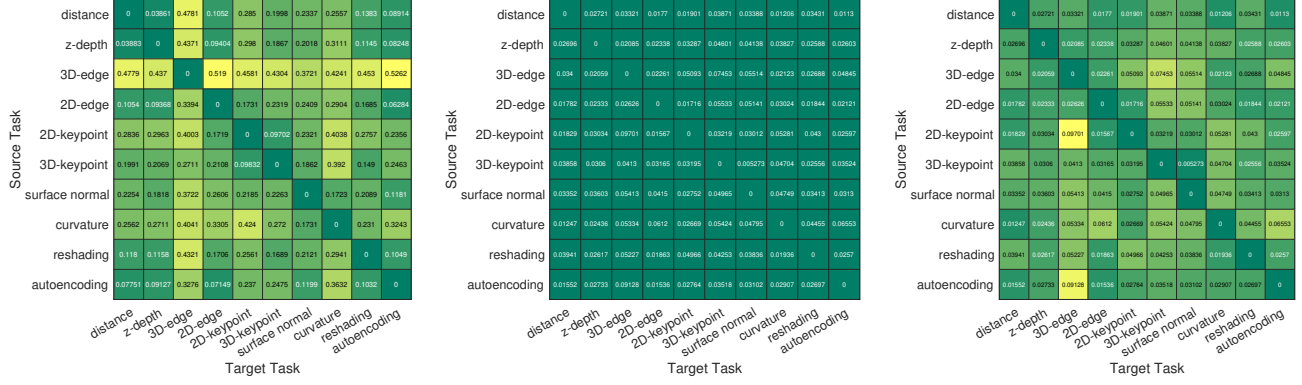


Figure 7: Distance from source tasks to the target tasks on Taskonomy data set found by our approach and Taskonomy transfer learning approach. The left panel shows the mean and the middle panel denotes the standard deviation values over 10 different trials. The right panel shows the task affinity found by transfer learning approach [54] after a single run.

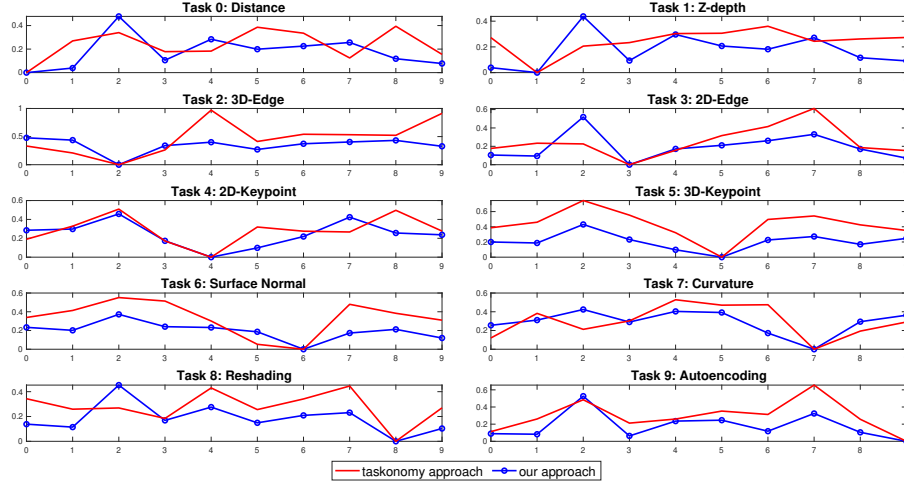


Figure 8: Comparison between our approach and Taskonomy [54] approach for each task.

In order to use the autoencoder for all the tasks without architecture modification, we convert all of the ground truth outputs to three channels. Figure 7 shows the mean (left panel) and the standard deviation (middle panel) of the task distance between each pair of tasks over 10 different initial settings in the training of the ε -approximation network. The right panel in Figure 7 shows the task affinity achieved by transfer learning in the Taskonomy paper for a single run. The task affinity found by the transfer learning approach does not give a clear boundary between tasks and may have a hard-time in identifying the closest tasks to some target tasks. Our approach, on the other hand is statistical and determines a clear boundary for the identification of related tasks based on the distance. Figure 8 illustrates the comparison between the distance to each task found by our approach and by the transfer learning approach in the Taskonomy paper. We note that both approaches follow a

similar trend for most of the tasks.

5. Conclusion

A task dissimilarity measure based on the Fréchet distance between Fisher Information Matrices is introduced in this paper. Using this measure, a reduced search space of architectures for a target task can be constructed using the closest task to the target from a set of baseline tasks. This reduces the complexity of architecture search, increases its efficiency, and leads to superior performance with a smaller number of parameters.

Acknowledgments

This work was supported by the Army Research Office grant No. W911NF-15-1-0479.

References

- [1] Alessandro Achille, Michael Lam, Rahul Tewari, Avinash Ravichandran, Subhansu Maji, Charles Fowlkes, Stefano Soatto, and Pietro Perona. Task2Vec: Task Embedding for Meta-Learning. *arXiv e-prints*, page arXiv:1902.03545, Feb. 2019.
- [2] Noor Awad, Neeratyoy Mallik, and Frank Hutter. Differential evolution for neural architecture search. *arXiv preprint arXiv:2012.06400*, 2020.
- [3] Gabriel Bender, Pieter-Jan Kindermans, Barret Zoph, Vijay Vasudevan, and Quoc Le. Understanding and simplifying one-shot architecture search. *Proc. Int. Conf. Machine Learning*, 2018.
- [4] Gabriel Bender, Hanxiao Liu, Bo Chen, Grace Chu, Shuyang Cheng, Pieter-Jan Kindermans, and Quoc V Le. Can weight sharing outperform random architecture search? an investigation with tunas. In *Proceedings of the IEEE/CVF Conference on Computer Vision and Pattern Recognition*, pages 14323–14332, 2020.
- [5] Han Cai, Tianyao Chen, Weinan Zhang, Yong Yu, and Jun Wang. Efficient architecture search by network transformation. *Proc. Assoc. Adv. Art. Intell. (AAAI)*, 2018.
- [6] Han Cai, Chuang Gan, Tianzhe Wang, Zhekai Zhang, and Song Han. Once-for-all: Train one network and specialize it for efficient deployment. *arXiv preprint arXiv:1908.09791*, 2019.
- [7] Han Cai, Ligeng Zhu, and Song Han. Proxylessnas: Direct neural architecture search on target task and hardware. *Proc. Int. Conf. Learning Representations*, 2019.
- [8] Wuyang Chen, Xinyu Gong, and Zhangyang Wang. Neural architecture search on imagenet in four gpu hours: A theoretically inspired perspective. *arXiv preprint arXiv:2102.11535*, 2021.
- [9] Minsu Cho, Mohammadreza Soltani, and Chinmay Hegde. One-shot neural architecture search via compressive sensing. *arXiv preprint arXiv:1906.02869*, 2019.
- [10] Xuanyi Dong and Yi Yang. Nas-bench-102: Extending the scope of reproducible neural architecture search. *arXiv preprint arXiv:2001.00326*, 2020.
- [11] K. Dwivedi and G. Roig. Representation similarity analysis for efficient task taxonomy and transfer learning. In *CVPR*. IEEE Computer Society, 2019.
- [12] Thomas Elsken, Jan Hendrik Metzen, and Frank Hutter. Efficient multi-objective neural architecture search via lamarckian evolution. *Proc. Int. Conf. Learning Representations*, 2019.
- [13] Chrisantha Fernando, Dylan Banarse, Charles Blundell, Yori Zwols, David Ha, Andrei A. Rusu, Alexander Pritzel, and Daan Wierstra. Pathnet: Evolution channels gradient descent in super neural networks. *CoRR*, abs/1701.08734, 2017.
- [14] Chelsea Finn, Xin Yu Tan, Yan Duan, Trevor Darrell, Sergey Levine, and Pieter Abbeel. Deep spatial autoencoders for visuomotor learning. In *Robotics and Automation (ICRA), 2016 IEEE International Conference on*, pages 512–519. IEEE, 2016.
- [15] S. Gadat and F. Panloup. Optimal non-asymptotic bound of the ruppert-polyak averaging without strong convexity. *arXiv preprint arXiv:1709.03342*, 2017.
- [16] Kaiming He, Xiangyu Zhang, Shaoqing Ren, and Jian Sun. Deep residual learning for image recognition. *IEEE Conf. Comp. Vision and Pattern Recog*, 2016.
- [17] Thibault Helleputte and Pierre Dupont. Feature selection by transfer learning with linear regularized models. In Wray Buntine, Marko Grobelnik, Dunja Mladenić, and John Shawe-Taylor, editors, *Machine Learning and Knowledge Discovery in Databases*, pages 533–547, Berlin, Heidelberg, 2009. Springer Berlin Heidelberg.
- [18] Hanzhang Hu, John Langford, Rich Caruana, Saurajit Mukherjee, Eric Horvitz, and Debadepta Dey. Efficient forward architecture search. *Adv. Neural Inf. Proc. Sys. (NeurIPS)*, 2019.
- [19] Gao Huang, Zhuang Liu, Laurens Van Der Maaten, and Kilian Q Weinberger. Densely connected convolutional networks. *IEEE Conf. Comp. Vision and Pattern Recog*, 2017.
- [20] Haifeng Jin, Qingquan Song, and Xia Hu. Efficient neural architecture search with network morphism. *arXiv preprint arXiv:1806.10282*, 2018.
- [21] Alex Krizhevsky, Geoffrey Hinton, et al. Learning multiple layers of features from tiny images. *Citeseer*, 2009.
- [22] Cat P Le, Mohammadreza Soltani, Robert Ravier, and Vahid Tarokh. Task-aware neural architecture search. *arXiv preprint arXiv:2010.13962*, 2020.
- [23] Yann LeCun, Corinna Cortes, and CJ Burges. Mnist handwritten digit database. *AT&T Labs [Online]*. Available: <http://yann.lecun.com/exdb/mnist>, 2:18, 2010.
- [24] Liam Li, Kevin Jamieson, Afshin Rostamizadeh, Ekaterina Gonina, Moritz Hardt, Benjamin Recht, and Ameet Talwalkar. Massively parallel hyperparameter tuning. *arXiv preprint arXiv:1810.05934*, 2018.
- [25] Liam Li and Ameet Talwalkar. Random search and reproducibility for neural architecture search. *arXiv preprint arXiv:1902.07638*, 2019.
- [26] Chenxi Liu, Barret Zoph, Maxim Neumann, Jonathon Shlens, Wei Hua, Li-Jia Li, Li Fei-Fei, Alan Yuille, Jonathan Huang, and Kevin Murphy. Progressive neural architecture search. *Euro. Conf. Comp. Vision*, 2018.
- [27] Hanxiao Liu, Karen Simonyan, and Yiming Yang. Darts: Differentiable architecture search. *Proc. Int. Conf. Machine Learning*, 2018.
- [28] Renqian Luo, Fei Tian, Tao Qin, Enhong Chen, and Tie-Yan Liu. Neural architecture optimization. *Adv. Neural Inf. Proc. Sys. (NeurIPS)*, 2018.
- [29] Zelun Luo, Yuliang Zou, Judy Hoffman, and Li F Fei-Fei. Label efficient learning of transferable representations across domains and tasks. In *Advances in Neural Information Processing Systems*, pages 164–176, 2017.
- [30] Arun Mallya and Svetlana Lazebnik. Piggyback: Adding multiple tasks to a single, fixed network by learning to mask. *CoRR*, abs/1801.06519, 2018.
- [31] Lilyana Mihalkova, Tuyen Huynh, and Raymond J Mooney. Mapping and revising markov logic networks for transfer learning. In *AAAI*, volume 7, pages 608–614, 2007.

- [32] Vu Nguyen, Tam Le, Makoto Yamada, and Michael A Osborne. Optimal transport kernels for sequential and parallel neural architecture search. *arXiv preprint arXiv:2006.07593*, 2020.
- [33] Alexandru Niculescu-Mizil and Rich Caruana. Inductive transfer for bayesian network structure learning. In *Artificial Intelligence and Statistics*, pages 339–346, 2007.
- [34] Asaf Noy, Niv Nayman, Tal Ridnik, Nadav Zamir, Sivan Doveh, Itamar Friedman, Raja Giryes, and Lihi Zelnik-Manor. Asap: Architecture search, anneal and prune. *arXiv preprint arXiv:1904.04123*, 2019.
- [35] Arghya Pal and Vineeth N Balasubramanian. Zero-shot task transfer, 2019.
- [36] S. J. Pan and Q. Yang. A survey on transfer learning. *IEEE Transactions on Knowledge and Data Engineering*, 22(10):1345–1359, Oct 2010.
- [37] Hieu Pham, Melody Y Guan, Barret Zoph, Quoc V Le, and Jeff Dean. Efficient neural architecture search via parameter sharing. *Proc. Int. Conf. Machine Learning*, 2018.
- [38] B. Polyak and A. Juditsky. Acceleration of stochastic approximation by averaging. *Siam Journal on Control and Optimization*, 30:838–855, 1992.
- [39] L. Y. Pratt. Discriminability-based transfer between neural networks. In S. J. Hanson, J. D. Cowan, and C. L. Giles, editors, *Advances in Neural Information Processing Systems 5*, pages 204–211. Morgan-Kaufmann, 1993.
- [40] Ali Sharif Razavian, Hossein Azizpour, Josephine Sullivan, and Stefan Carlsson. Cnn features off-the-shelf: An astounding baseline for recognition. In *Proceedings of the 2014 IEEE Conference on Computer Vision and Pattern Recognition Workshops, CVPRW '14*, pages 512–519, Washington, DC, USA, 2014. IEEE Computer Society.
- [41] Esteban Real, Alok Aggarwal, Yanping Huang, and Quoc V Le. Regularized evolution for image classifier architecture search. *Proc. Assoc. Adv. Art. Intell. (AAAI)*, 2019.
- [42] Olga Russakovsky, Jia Deng, Hao Su, Jonathan Krause, Sanjeev Satheesh, Sean Ma, Zhiheng Huang, Andrej Karpathy, Aditya Khosla, Michael Bernstein, Alexander C. Berg, and Li Fei-Fei. ImageNet Large Scale Visual Recognition Challenge. *International Journal of Computer Vision (IJCV)*, 115(3):211–252, 2015.
- [43] Andrei A. Rusu, Neil C. Rabinowitz, Guillaume Desjardins, Hubert Soyer, James Kirkpatrick, Koray Kavukcuoglu, Razvan Pascanu, and Raia Hadsell. Progressive neural networks. *CoRR*, abs/1606.04671, 2016.
- [44] Christian Scuto, Kaicheng Yu, Martin Jaggi, Claudiu Musat, and Mathieu Salzmann. Evaluating the search phase of neural architecture search. *arXiv preprint arXiv:1902.08142*, 2019.
- [45] Daniel L Silver and Kristin P Bennett. Guest editor’s introduction: special issue on inductive transfer learning. *Machine Learning*, 73(3):215–220, 2008.
- [46] Karen Simonyan and Andrew Zisserman. Very deep convolutional networks for large-scale image recognition. *arXiv preprint arXiv:1409.1556*, 2014.
- [47] Xingyou Song, Krzysztof Choromanski, Jack Parker-Holder, Yunhao Tang, Daiyi Peng, Deepali Jain, Wenbo Gao, Aldo Pacchiano, Tamas Sarlos, and Yuxiang Yang. Es-enas: Combining evolution strategies with neural architecture search at no extra cost for reinforcement learning. *arXiv preprint arXiv:2101.07415*, 2021.
- [48] Trevor Standley, Amir Zamir, Dawn Chen, Leonidas Guibas, Jitendra Malik, and Silvio Savarese. Which tasks should be learned together in multi-task learning? In Hal Daumé III and Aarti Singh, editors, *Proceedings of the 37th International Conference on Machine Learning*, volume 119 of *Proceedings of Machine Learning Research*, pages 9120–9132. PMLR, 13–18 Jul 2020.
- [49] Y. Sun, X. Sun, Y. Fang, G. G. Yen, and Y. Liu. A novel training protocol for performance predictors of evolutionary neural architecture search algorithms. *IEEE Transactions on Evolutionary Computation*, pages 1–1, 2021.
- [50] Alvin Wan, Xiaoliang Dai, Peizhao Zhang, Zijian He, Yuan-dong Tian, Saining Xie, Bichen Wu, Matthew Yu, Tao Xu, Kan Chen, et al. Fbnetv2: Differentiable neural architecture search for spatial and channel dimensions. In *Proceedings of the IEEE/CVF Conference on Computer Vision and Pattern Recognition*, pages 12965–12974, 2020.
- [51] Aria Y Wang, Leila Wehbe, and Michael J Tarr. Neural taskonomy: Inferring the similarity of task-derived representations from brain activity. *BioRxiv*, page 708016, 2019.
- [52] Sirui Xie, Hehui Zheng, Chunxiao Liu, and Liang Lin. Snas: stochastic neural architecture search. *arXiv preprint arXiv:1812.09926*, 2018.
- [53] Zhaohui Yang, Yunhe Wang, Xinghao Chen, Boxin Shi, Chao Xu, Chunjing Xu, Qi Tian, and Chang Xu. Cars: Continuous evolution for efficient neural architecture search. In *Proceedings of the IEEE/CVF Conference on Computer Vision and Pattern Recognition*, pages 1829–1838, 2020.
- [54] Amir R Zamir, Alexander Sax, William B Shen, Leonidas Guibas, Jitendra Malik, and Silvio Savarese. Taskonomy: Disentangling task transfer learning. In *2018 IEEE Conference on Computer Vision and Pattern Recognition (CVPR)*. IEEE, 2018.
- [55] Miao Zhang, Huiqi Li, Shirui Pan, Xiaojun Chang, and Steven Su. Overcoming multi-model forgetting in one-shot nas with diversity maximization. In *Proceedings of the IEEE/CVF Conference on Computer Vision and Pattern Recognition*, pages 7809–7818, 2020.
- [56] Yiyang Zhao, Linnan Wang, Yuandong Tian, Rodrigo Fonseca, and Tian Guo. Few-shot neural architecture search. *arXiv preprint arXiv:2006.06863*, 2020.
- [57] Dongzhan Zhou, Xinchu Zhou, Wenwei Zhang, Chen Change Loy, Shuai Yi, Xuesen Zhang, and Wanli Ouyang. Ecnas: Finding proxies for economical neural architecture search. In *Proceedings of the IEEE/CVF Conference on Computer Vision and Pattern Recognition*, pages 11396–11404, 2020.
- [58] Barret Zoph and Quoc V Le. Neural architecture search with reinforcement learning. *Proc. Int. Conf. Learning Representations*, 2017.
- [59] Barret Zoph, Vijay Vasudevan, Jonathon Shlens, and Quoc V Le. Learning transferable architectures for scalable image recognition. *IEEE Conf. Comp. Vision and Pattern Recog*, 2018.

A. Detail of Experiments

In our experiments, the first step is to train the ϵ -approximation network with the balanced data from each task. For classification tasks (e.g., tasks in MNIST [23], CIFAR-10 [21], CIFAR-100 [21], ImageNet [42]), three different architectures, including VGG-16 [46], Resnet-18 [16], DenseNet-121 [19], are chosen as ϵ -approximation network. The training procedure is conducted in 100 epochs, with Adam optimizer. The batch size is set to 128. For image processing tasks in Taskonomy [54], we use an autoencoder as the ϵ -approximation network. The part of the autoencoder consists of one convolutional layer, and two linear layers. The convolutional layer has 3 input channels and 16 output channels with the kernel size equals to 5. We also use the zero padding of size 2, stride of size 4, and dilation equals to 1. The first linear layer has the size of (262144, 512), and the second linear layer has the size of (512, 128). The training procedure is conducted in 20 epochs with Adam optimizer, a batch size of 64, and mean-square error loss.

In order to construct the dictionary for baseline tasks, we need to perform the architecture search for these tasks using general search space. This space is defined by cells structure, consisting of 3 or 4 nodes, and 10 operations (i.e., zero, identity, maxpool3x3, avepool3x3, conv3x3, conv5x5, conv7x7, dil-conv3x3, dil-conv5x5, conv7x1-1x7). After the best cell for each baseline task is founded, we save the structures and operations to the dictionary.

The source code for the experiments is available at: <https://github.com/lephuoccat/Fisher-Information-NAS>. Next, we provide the the proof of the theorem 1 and the theorem 2.

B. Proof of Theorem 1

Theorem 1. *Let X be the data set for the target task T . Consider two structurally-similar ϵ -approximation networks w.r.t. (T, X) , N_1 and N_2 with the set of weights θ_1 and θ_2 trained using the SGD algorithm where a diminishing learning rate is used for updating weights. Assume that the loss function L for the task T is strongly convex, and its 3rd-order continuous derivative exists and bounded. Let the noisy gradient function in training N_1 and N_2 networks using SGD algorithm be given by:*

$$g(\theta_{it}, \epsilon_{it}) = \nabla L(\theta_{it}) + \epsilon_{it}, \text{ for } i = 1, 2, \quad (9)$$

where θ_{it} is the estimation of the weights for network N_i at time t , and $\nabla L(\theta_{it})$ is the true gradient at θ_{it} . Assume that ϵ_{it} satisfies $\mathbb{E}[\epsilon_{it} | \epsilon_{i0}, \dots, \epsilon_{it-1}] = 0$, and satisfies $s = \lim_{t \rightarrow \infty} \mathbb{E}[\|\epsilon_{it}\epsilon_{it}^T | \epsilon_{i0}, \dots, \epsilon_{it-1}\|]_{\infty} < \infty$ almost surely (a.s.). Then the Fréchet distance between N_1 and N_2 computed on the average of estimated weights up to the current

time t converges to zero as $t \rightarrow \infty$. That is,

$$d_t = \frac{1}{\sqrt{2}} \left\| \bar{F}_{1t}^{1/2} - \bar{F}_{2t}^{1/2} \right\|_F \xrightarrow{\mathcal{D}} 0, \quad (10)$$

where $\bar{F}_{it} = F(\bar{\theta}_{it})$ with $\bar{\theta}_{it} = \frac{1}{t} \sum_t \theta_{it}$, for $i = 1, 2$.

Proof of Theorem 1. Here, we show the proof for the full Fisher Information Matrix; however, the same results holds for the diagonal approximation of the Fisher Information Matrix. Let N_1 with weights θ_1 and N_2 with weights θ_2 be the two structurally-similar ϵ -approximation networks w.r.t. (T, X) . Let n be the number of trainable parameters in N_1 and N_2 . Since the objective function is strongly convex and the fact that N_1 and N_2 are structurally-similar ϵ -approximation networks w.r.t. (T, X) , both of these network will obtain the optimum solution θ^* after training a certain number of epochs with stochastic gradient descend. By the assumption on the conditional mean of the noisy gradient function and the assumption on S , the conditional covariance matrix is finite as well, i.e., $C = \lim_{t \rightarrow \infty} \mathbb{E}[\epsilon_{it}\epsilon_{it}^T | \epsilon_{i0}, \dots, \epsilon_{it-1}] < \infty$; hence, we can invoke the following result due to Polyak et al. [38]:

$$\sqrt{t}(\bar{\theta}_t - \theta^*) \xrightarrow{\mathcal{D}} \mathcal{N}\left(0, \mathbf{H}(L(\theta^*))^{-1} C \mathbf{H}^T(L(\theta^*))^{-1}\right), \quad (11)$$

as $t \rightarrow \infty$. Here, \mathbf{H} is Hessian matrix, θ^* is the global minimum of the loss function, and $\bar{\theta}_t = \frac{1}{t} \sum_t \theta_t$. Hence, for networks N_1 and N_2 and from Equation (11), $\sqrt{t}(\bar{\theta}_{1t} - \theta^*)$ and $\sqrt{t}(\bar{\theta}_{2t} - \theta^*)$ are asymptotically normal random vectors:

$$\sqrt{t}(\bar{\theta}_{1t} - \theta^*) \xrightarrow{\mathcal{D}} \mathcal{N}(0, \Sigma_1), \quad (12)$$

$$\sqrt{t}(\bar{\theta}_{2t} - \theta^*) \xrightarrow{\mathcal{D}} \mathcal{N}(0, \Sigma_2), \quad (13)$$

where $\Sigma_1 = \mathbf{H}(L(\theta^*))^{-1} C_1 \mathbf{H}^T(L(\theta^*))^{-1}$, and $\Sigma_2 = \mathbf{H}(L(\theta^*))^{-1} C_2 \mathbf{H}^T(L(\theta^*))^{-1}$. The Fisher Information $F(\theta)$ is a continuous and differentiable function of θ . Since it is also a positive definite matrix, $F(\theta)^{1/2}$ is well-defined. Hence, by applying the Delta method to Equation (12), we have:

$$\sqrt{t}(\bar{F}_{1t}^{1/2} - F^{*1/2}) \xrightarrow{\mathcal{D}} \mathcal{N}(0, \Sigma_1^*), \quad (14)$$

where $\bar{F}_{1t} = F(\bar{\theta}_{1t})$, and the covariance matrix Σ_1^* is given by $\Sigma_1^* = \mathbf{J}_{\theta}(\text{vec}(F(\theta^*)^{1/2})) \Sigma_1 \mathbf{J}_{\theta}(\text{vec}(F(\theta^*)^{1/2}))^T$. Here, $\text{vec}()$ is the vectorization operator, θ^* is a $n \times 1$ vector of the optimum parameters, $F(\theta^*)$ is a $n \times n$ Matrix evaluated at the minimum, and $\mathbf{J}_{\theta}(F(\theta^*))$ is a $n^2 \times n$ Jacobian matrix of the Fisher Information Matrix. Similarly, from Equation (13), we have:

$$\sqrt{t}(\bar{F}_{2t}^{1/2} - F^{*1/2}) \xrightarrow{\mathcal{D}} \mathcal{N}(0, \Sigma_2^*), \quad (15)$$

where $\Sigma_2^* = \mathbf{J}_\theta \left(\text{vec}(F(\theta^*)^{1/2}) \right) \Sigma_2 \mathbf{J}_\theta \left(\text{vec}(F(\theta^*)^{1/2}) \right)^T$. As a result, $(\bar{F}_{1t}^{1/2} - \bar{F}_{2t}^{1/2})$ is asymptotically a normal random vector:

$$(\bar{F}_{1t}^{1/2} - \bar{F}_{2t}^{1/2}) \xrightarrow{\mathcal{D}} \mathcal{N}(0, V_1). \quad (16)$$

where $V_1 = \frac{1}{t}(\Sigma_1^* + \Sigma_2^*)$. As t approaches infinity, $\frac{1}{t}(\Sigma_1^* + \Sigma_2^*) \rightarrow 0$. As a result, $d_t = \frac{1}{\sqrt{2}} \left\| \bar{F}_{1t}^{1/2} - \bar{F}_{2t}^{1/2} \right\|_F \xrightarrow{\mathcal{D}} 0$. \square

C. Proof of Theorem 2

Theorem 2. Let X_A be the data set for the task T_A with the objective function L_A , and X_B be the data set for the task T_B with the objective function L_B . Assume X_A and X_B have the same distribution. Consider an ε -approximation network N trained using both data sets $X_A^{(1)}$ and $X_B^{(1)}$ respectively with the objective functions L_A and L_B to result weights θ_{At} and θ_{Bt} at time t . Under the same assumptions on the moment of gradient noise in SGD algorithm and the loss function stated in Theorem 1, the Fréchet distance from the task A to the task B computed from the Fisher Information Matrix of the average of estimated weights up to the current time t converges to a constant as $t \rightarrow \infty$. That is,

$$d_t = \frac{1}{\sqrt{2}} \left\| \bar{F}_{At}^{1/2} - \bar{F}_{Bt}^{1/2} \right\|_F \xrightarrow{\mathcal{D}} \frac{1}{\sqrt{2}} \left\| F_A^{*1/2} - F_B^{*1/2} \right\|_F, \quad (17)$$

where \bar{F}_{At} is given by $\bar{F}_{At} = F(\bar{\theta}_{At})$ with $\bar{\theta}_{At} = \frac{1}{t} \sum_t \theta_{At}$, and \bar{F}_{Bt} is defined in an analogous manner.

Proof of Theorem 2. Let θ_{At} and θ_{Bt} be the sets of weights at time t from the ε -approximation network N trained using both data sets $X_A^{(1)}$ and $X_B^{(1)}$, respectively with the objective functions L_A and L_B . Since the objective functions are strongly convex, both of these sets of weights will obtain the optimum solutions θ_A^* and θ_B^* after training a certain number of epochs with stochastic gradient descend. Similar to the proof of Theorem 1, by invoking the Polyak et al. [38], random vectors of $\sqrt{t}(\bar{\theta}_{At} - \theta_A^*)$ and $\sqrt{t}(\bar{\theta}_{Bt} - \theta_B^*)$ are asymptotically normal:

$$\sqrt{t}(\bar{\theta}_{At} - \theta_A^*) \xrightarrow{\mathcal{D}} \mathcal{N}(0, \Sigma_A), \quad (18)$$

$$\sqrt{t}(\bar{\theta}_{Bt} - \theta_B^*) \xrightarrow{\mathcal{D}} \mathcal{N}(0, \Sigma_B), \quad (19)$$

where $\Sigma_A = \mathbf{H}(L(\theta_A^*))^{-1} C_A \mathbf{H}^T(L(\theta_A^*))^{-1}$, and $\Sigma_B = \mathbf{H}(L(\theta_B^*))^{-1} C_B \mathbf{H}^T(L(\theta_B^*))^{-1}$ (here, C_A and C_B denote the conditional covariance matrices, corresponding to the gradient noise in θ_A^* and θ_B^* , respectively). The Fisher Information $F(\theta)$ is a continuous and differentiable function of θ , and it is also a positive definite matrix; thus, $F(\theta)^{1/2}$ is

well-defined. Now, by applying the Delta method to Equation (18), we have:

$$(\bar{F}_{At}^{1/2} - F_A^{*1/2}) \xrightarrow{\mathcal{D}} \mathcal{N}\left(0, \frac{1}{t} \Sigma_A^*\right), \quad (20)$$

where $\bar{F}_{At} = F(\bar{\theta}_{At})$, and the covariance matrix is given by $\Sigma_A^* = \mathbf{J}_\theta \left(\text{vec}(F(\theta_A^*)^{1/2}) \right) \Sigma_A \mathbf{J}_\theta \left(\text{vec}(F(\theta_A^*)^{1/2}) \right)^T$. Likewise, from Equation (19), we have:

$$(\bar{F}_{Bt}^{1/2} - F_B^{*1/2}) \xrightarrow{\mathcal{D}} \mathcal{N}\left(0, \frac{1}{t} \Sigma_B^*\right), \quad (21)$$

where $\bar{F}_{Bt} = F(\bar{\theta}_{Bt})$, and the covariance matrix is given by $\Sigma_B^* = \mathbf{J}_\theta \left(\text{vec}(F(\theta_B^*)^{1/2}) \right) \Sigma_B \mathbf{J}_\theta \left(\text{vec}(F(\theta_B^*)^{1/2}) \right)^T$. From Equation (20) and (21), we obtain:

$$(\bar{F}_{At}^{1/2} - \bar{F}_{Bt}^{1/2}) \xrightarrow{\mathcal{D}} \mathcal{N}(\mu_2, V_2), \quad (22)$$

where $\mu_2 = (F_A^{*1/2} - F_B^{*1/2})$ and $V_2 = \frac{1}{t}(\Sigma_A^* + \Sigma_B^*)$. Since $(\bar{F}_{At}^{1/2} - \bar{F}_{Bt}^{1/2}) - (F_A^{*1/2} - F_B^{*1/2})$ is asymptotically normal with the covariance goes to zero as t approaches infinity, all of the entries go to zero, we conclude that

$$d_t = \frac{1}{\sqrt{2}} \left\| \bar{F}_{At}^{1/2} - \bar{F}_{Bt}^{1/2} \right\|_F \xrightarrow{\mathcal{D}} \frac{1}{\sqrt{2}} \left\| F_A^{*1/2} - F_B^{*1/2} \right\|_F. \quad (23)$$

\square